

Interdepartmental letterhead

Mail Station L- 43  
Ext: 3-4801

RP-85-91

August 2, 1985

MEMORANDUM

TO: Distribution  
FROM: M. E. Glinsky MEG  
SUBJECT: Mica Rocking Curves

---

Attached is a report on the data collected up to this time on Mica.

Work is currently under way to measure the single crystal rocking curve using a neon gas absorption cell illuminated by the Ni L- $\beta$  line at 870 eV. This source will also be used to measure the resolution of a curved mica crystal.

If time permits the temperature dependence of the single crystal rocking curve will be measured between 300 and 500°K.

MEG:tm

Distribution:

C. Anderson  
R. Buck  
G. Chandler  
W. Cooper  
R. Lear  
H. Mallett  
J. Morgan  
C. Poppe  
A. Toor

R-Project Group  
X-Ray Measurements

University of California

 Lawrence Livermore  
National Laboratory

# Resolving Power of Muscovite Mica (002)

by  
M. E. Glinsky  
P. A. Waide

## ABSTRACT

Single crystal integrated reflectivity and double crystal (1,-1) rocking curve were measured for muscovite mica (002) at 930 eV. The measured and calculated values for  $R_c$ , the single crystal integrated reflectivity,  $R$ , the double crystal integrated reflectivity,  $P$ , the maximum double crystal reflectivity, and  $W$ , the FWHM of the double crystal rocking curve are:

	<u>Measured</u>	<u>Calculated</u>	
$R_c$	$2.27 \pm 0.40$	1.29	$\times 10^{-5}$ rad
$R$	$3.43 \pm 0.21$	2.52	$\times 10^{-5}$ rad
$P$	$0.017 \pm 0.0011$	0.0178	
$W$	1.5	1.10	$\times 10^{-3}$ rad

The calculated values were derived from the Darwin-Prins dynamical theory of X-ray diffraction using the program ROCKIT. The resolving power implied by these numbers is between 1300 and 1800 at 930 eV.

## INTRODUCTION

In order to put limits on the resolving power of muscovite mica (002), the double crystal rocking curve was measured and compared to the theoretical result of the Darwin-Prins dynamical theory of X-ray diffraction {1,2}. The geometry used for the double crystal rocking curve was the energy non-dispersive (1,-1) arrangement shown in figure 1b. The reflectivity of the second crystal as a function of  $\partial'$ , the deviation from the bragg angle, is independent of the vertical or angular divergence of the incident X-ray beam when this geometry is used {3}. In fact it is the convolution of the single crystal rocking curve,  $f(\partial)$ , with itself, as given in the following equation.

$$F(\partial') = \frac{\int_{-\infty}^{\infty} f_{\Sigma}(\partial) * f_{\Sigma}(\partial'-\partial) d\partial + \int_{-\infty}^{\infty} f_{\pi}(\partial) * f_{\pi}(\partial'-\partial) d\partial}{\int_{-\infty}^{\infty} f_{\Sigma}(\partial) d\partial + \int_{-\infty}^{\infty} f_{\pi}(\partial) d\partial} \quad (1)$$

$f_{\pi}(\partial)$  is the single crystal rocking curve for parallel polarized X-rays and  $f_{\Sigma}(\partial)$  is the single crystal rocking curve for normal polarized X-rays. The single crystal rocking curve is defined in figure 1a. It is the reflectivity of the crystal as a function of deviation from the bragg angle for monoenergetic X-rays.

The single crystal integrated reflectivity,  $R_c$ , is defined as follows:

$$R_c = \frac{1}{2} \int_{-\infty}^{\infty} f_{\Sigma}(\partial) d\partial + \frac{1}{2} \int_{-\infty}^{\infty} f_{\pi}(\partial) d\partial = \frac{I(\partial)}{I_0} \quad (2)$$

$I_0$  is the total intensity of the incoming X-ray beam.  $I(\partial)$  is the reflected intensity.  $R_c$  is independent of energy dispersion of the crystal or vertical and horizontal divergence of the incoming X-ray beam, given that  $f(\partial)$  is constant over the energy range of the X-ray beam {4}. The independence of both  $R_c$  and  $F(\partial')$  from the characteristics of the incoming X-ray beam make them easy to measure in the laboratory.

If there are no defects in the crystalline structure, the function  $f(\partial)$  is predicted quite well by the dynamical theory of X-ray

diffraction. The presence of defects causes mosaic structure in the crystal. Mosaic structure is a theoretical construct that assumes that there are regions of the crystal with perfect structure that have a mean radius,  $r$ . These regions are assumed to be aligned around an angle,  $\beta_0$ , with a distribution given by

$$W(\beta) = \frac{1}{\sqrt{2\pi}\sigma} e^{-\frac{(\beta-\beta_0)^2}{2\sigma^2}} \quad (3)$$

The effect of mosaic structure on  $f(\theta)$  is to give it the shape and width of  $W(\beta-\beta_0)$  and to increase the integrated reflectivity,  $R_c$ , up to a maximum value of

$$R_c^{\text{mosaic}} = \left[ \frac{e^2 |F_H|}{m_e c^2 V} \right]^2 \frac{\lambda^3}{2\mu_0} \frac{1 + \cos^2 2\theta_B}{2 \sin 2\theta_B} \quad (4)$$

$V$  = volume of unit cell

$F_H$  = form factor for reflection from plane H

$\mu_0$  = mass attenuation coefficient

for an ideally mosaic crystal {5}.

The resolving power for some spectrometer designs is dependent on the width of the rocking curve for the individual perfect domains not the rocking curve for the crystal as a whole {6}. In fact, it is desirable to have a crystal with significant mosaic structure so that it has a high integrated reflectivity, reflecting a large amount of the incident X-ray beam. The resolution of the instrument will not be degraded by the mosaic broadening of the total crystal rocking curve, if the resolution only depends on the angular divergence of the reflected beam determined by the response of the perfect domains.

The question that is being addressed by this investigation is how much mosaic broadening and increase in integrated reflectivity is there over what would be predicted for a perfect mica crystal.

## EXPERIMENTAL

Muscovite mica cleaved along the 002 plane to a thickness of 0.13 mm and cut in a square 3.8 x 3.8 cm was used. The thin sheet of mica is optically contacted to a glass flat so that the deviation in the angle of its surface is less than  $3 \times 10^{-4}$  rad.

To obtain the single crystal integrated reflectivity,  $R_c$ , the geometrical setup shown in figure 2a was used. The X-rays were generated by a Henke source with a copper anode. The potential of the anode was 2.5 KV and the anode current varied between 0.5 and 15 mA. The system was maintained at a pressure of  $5 \times 10^{-6}$  torr. The angular divergence for the single crystal measurements was  $5 \times 10^{-4}$  rad in the horizontal direction and 20 mrad in the vertical direction. A gas proportional counter maintained at a pressure of 350 torr was used to detect the X-rays. The incident intensity of the L-alpha and L-beta lines was taken and used to normalize the spectrum generated by scanning the crystal through a range of bragg angles that encompassed the same lines. The integral of this spectrum was calculated to yield a value for  $R_c$ .

The double crystal curve,  $F(\vartheta')$ , was measured using the geometry shown in figure 2b. The angle of the first crystal,  $\vartheta$ , was set to the peak of the L-alpha line at 930 eV and the second crystal was rotated to generate  $F(\vartheta')$ . The same acquisition parameters were used as in the case of the single crystal rocking curve except the horizontal divergence was increased to 6 mrad.

## RESULTS

The spectrum of the copper L-alpha (929.7 eV) and L-beta (949.8 eV) lines appears in figure 3. The integrated intensities of the two lines is  $2.27 \pm 0.40 \times 10^{-5}$  rad compared to the calculated value for  $R_c$  of  $1.29 \times 10^{-5}$  rad. This increase in integrated reflectivity can not be explained by mosaic structure since the maximum  $R_c$  predicted by equation 4 is  $1.36 \times 10^{-5}$  rad.

The measured double crystal rocking curve is shown in figure 4 and is compared  $F(\vartheta')$  for a perfect mica crystal. Although the peak

reflectivity of the two curves are the same, the width of the measured curve is  $1.5 \times 10^{-3}$  rad compared to the calculated value of  $1.1 \times 10^{-3}$  rad. The measured integrated reflectivity,  $R = 3.43 \pm 0.21 \times 10^{-5}$  rad, is correspondingly larger than the calculated value of  $2.52 \times 10^{-5}$  rad.

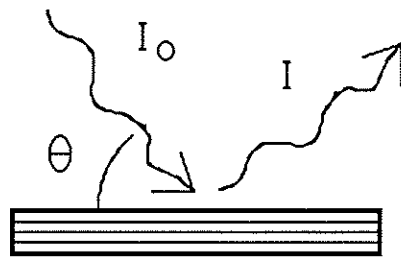
## CONCLUSIONS

The double crystal rocking curve for mica is broadened ~50% by mosaic structure. The calculated single crystal rocking curve appears in figure 5. The resolving power shown by this curve is 1800 at 930 eV. The resolving power implied by the measured width of  $F(\theta')$  is 1300. These two numbers give a good upper and lower bound to the resolving power that can be expected from mica. The appropriate value is dependent on whether the resolving power of the individual domains or the crystal as a whole is being used by the spectrometer geometry.

## REFERENCES

1. Zachariasen, W. H.: Theory of X-ray Diffraction in Crystals, Wiley New York, 1946, pp. 82-155.
2. Glinsky, M. E.: ROCKIT User's Guide, RP-85-90, 1985.
3. Compton, A. H., Allison, S. K.: X-rays in Theory and Experiment, Van Nostrand Princeton, 1935, pp. 718-730.
4. Burek, A. J.: Crystals for Astronomical X-ray Spectroscopy, LA-UR-75-1593, 1975, pp. 9-10.
5. Zachariasen, W. H.: Theory of X-ray Diffraction in Crystals, Wiley New York, 1946, pp. 156-176.
6. Angel, J. R. P., Weisskopf, M. C.: Astronomical Journal **75**, 231-236 (1970).

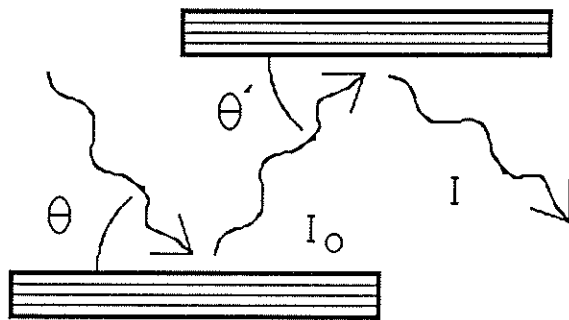
Figure 1a.



$$\vartheta = \theta - \theta_B$$

single crystal rocking curve =  $f(\vartheta) = I / I_0$

Figure 1b.



$$\vartheta' = \theta' - \theta'_B$$

double crystal rocking curve =  $F(\vartheta') = I / I_0$



Figure 2a.

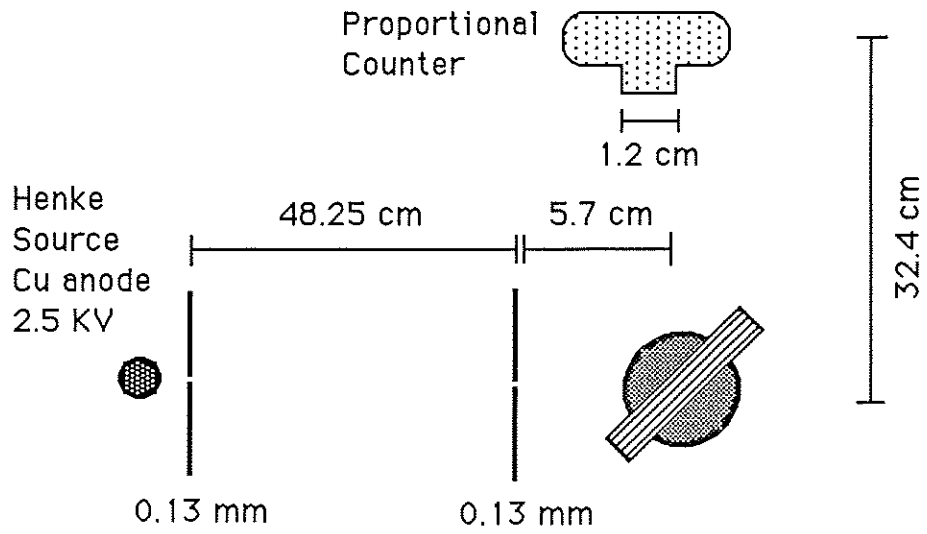
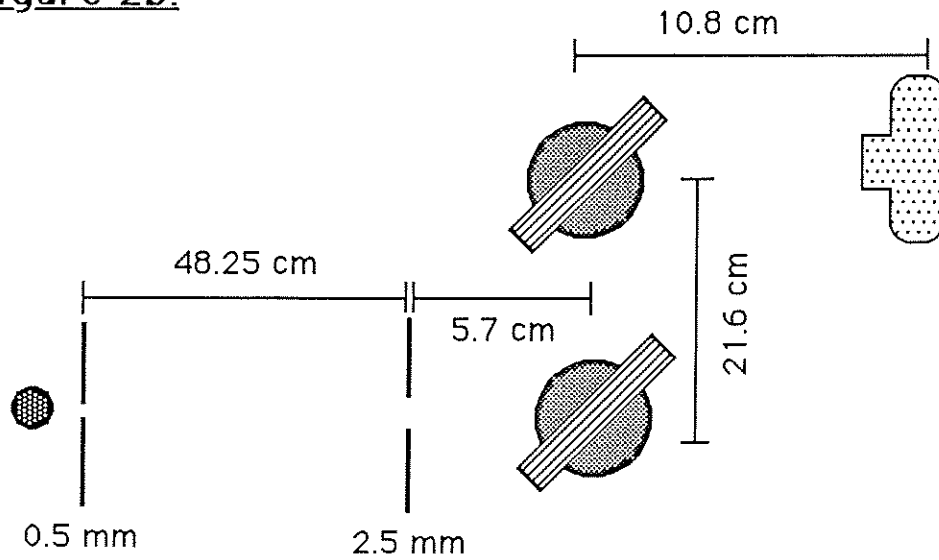


Figure 2b.



**Figure 3.**

SINGLE MICA CRYSTAL REFLECTION (COPPER L-ALPHA L-BETA)

FILES XTAL

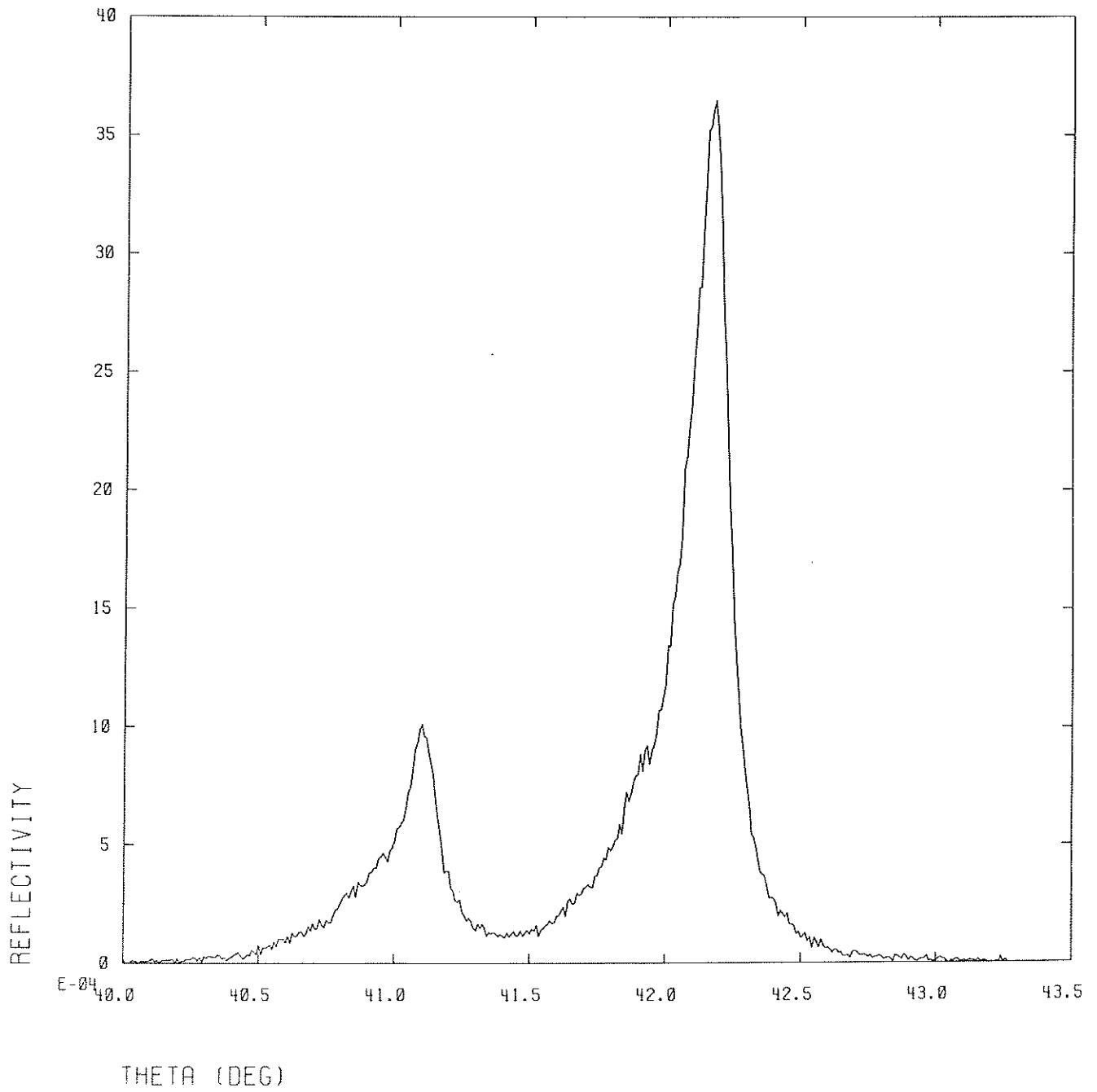


**Figure 4.**

MICA DOUBLE CRYSTAL ROCKING CURVE (1,-1) AT 930 EV

FILES EXPERIMENT (T., THEORY)

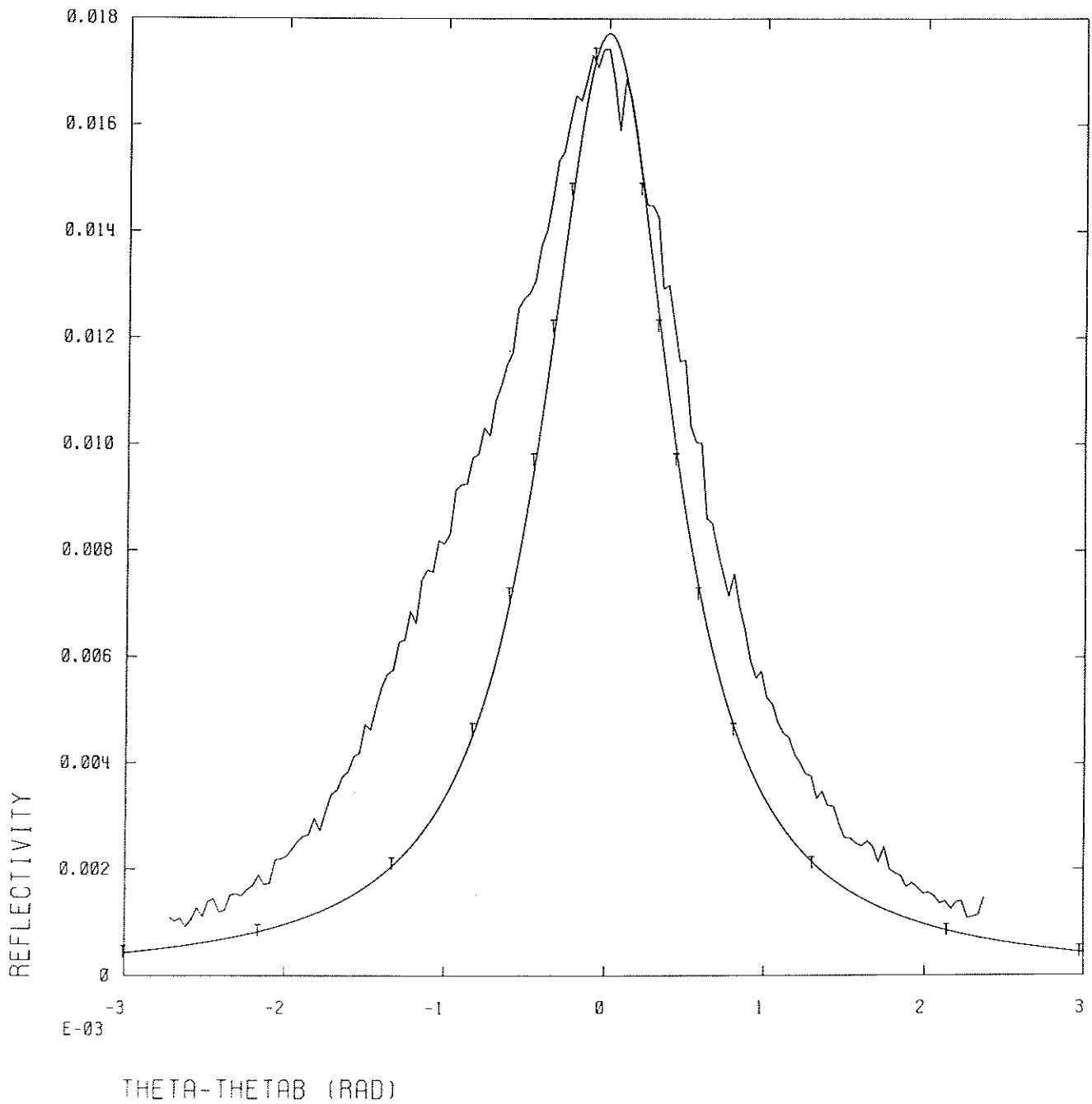


**Figure 5.**

CALCULATED MICA SINGLE CRYSTAL ROCKING CURVE AT 930 EV

FILES      AVERAGE

